Ion-beam mixing of Ag/Fe and In/Fe layers studied by hyperfine techniques

M. Neubauer, K. P. Lieb, P. Schaaf, and M. Uhrmacher
II. Physikalisches Institut and Sonderforschungsbereich 345, Universität Göttingen, Bunsenstraße 7-9, D-37073 Göttingen, Germany
(Received 11 July 1995)

Ion-beam mixing of the thermally immiscible systems Fe/Ag and Fe/In by 450- and 600-keV Xe ions was investigated by means of perturbed angular correlation (PAC) and conversion electron Mössbauer spectroscopy. The ^{111}In PAC probe atoms were either implanted into the layers at 400 keV or deposited by evaporation at the metal-metal interface. Using these different methods of doping it was possible to distinguish between the mixing process at the interface and ''long-range'' effects. Different magnetic hyperfine fields associated with one or two Ag atoms close to the hyperfine probe were identified via both hyperfine methods. The results are compared with those of a supersaturated homogeneous Fe(Ag) alloy.

I. INTRODUCTION

In recent years detailed studies of ion-beam mixing in metallic layers have been carried out, especially in systems with a negative heat of mixing ($\Delta H_{\rm mix}<0$). These investigations have led to refined models of the ion-beam-induced atomic transport through the interface(s).[1] It turned out that the ballistic model of Sigmund and Gras-Marti,[2,3] which essentially associates atomic transport with the energy deposited in the interface (F_D), predicts a mixing rate that is up to ten times smaller than the one measured in most miscible systems. Moreover, mixing was found to increase with increasing $\Delta H_{\rm mix}$ and decreasing cohesive energy ($\Delta H_{\rm coh}$). Such chemical driving forces can be explained if the ion impact results in a ''collective'' excitement of the solid along the ion path and is attributed to thermal spike formation. Several thermal spike models have been proposed but for most of the investigated systems the description in terms of a local spike model was most successful.[1,4] According to Cheng,[5] a necessary condition for the formation of a thermal spike is that the mean atomic number ($\bar{Z}$) of the target material exceeds $\bar{Z}=20$. In all these models it has thus been assumed that the chemical driving forces are favorable to the mixing in miscible systems, i.e., $\Delta H_{\rm mix}<0$. For systems with positive heat of mixing, $\Delta H_{\rm mix}>0$, little experimental work has been done so far.

For the present study, the systems Ag/Fe and In/Fe with their large positive $\Delta H_{\rm mix}$ were chosen. The models predict the formation of thermal spikes ($\bar{Z}>20$) for these systems. The opposite effects of (ballistic) mixing and local demixing in thermal spikes are expected to be active at the interface, leading to a complicated atomic transport pattern. To investigate these competing effects, the methods of perturbed angular correlation (PAC) and Conversion Electron Mössbauer spectroscopy (CEMS) were chosen because of their high sensitivity to the microsurrounding of the probe atoms.

In the miscible systems Al/Ni and Sb/Ni it has previously been shown that PAC measurements are appropriate to provide detailed information on the early stage of the mixing and the phase formation process.[6,7] Mössbauer spectroscopy is well suited to observe such effects for metallic multilayers containing, for example, iron.[8]

II. EXPERIMENTAL DETAILS

Thin Fe and Ag films (typically 50–100 nm each) were deposited by electron-gun or thermal evaporation at a rate of 0.3 nm/s onto Si wafers at room temperature. The In films were deposited at 90 K. The base pressure in the vacuum chamber was 6×10^{-5} Pa, rising to about 5×10^{-4} Pa during deposition. The thickness of the layers was measured by a quartz oscillator and checked using Rutherford backscattering spectroscopy (RBS).

For a series of PAC measurements some 10^{12} radioactive ^{111}In atoms were deposited at the interface between the metallic layers. In these cases the ^{111}In was immediately evaporated from a thin tungsten wire after the deposition of the Fe layer and promptly covered with a layer of Ag, In, or Fe without breaking the vacuum. The other samples were prepared by implanting the ^{111}In tracers at 400 keV at room temperature into the layer stacks. Due to the small but not exactly known $^{111}In^{+}$ beam spot size, the fluence might have reached up to 10^{14} ions/cm^2 in some experiments.

Afterwards, the samples were irradiated with 240, 450, or 600 keV Xe ions, up to a dose of 10^{16} Xe/cm^2. All Xe irradiations were done at 77 K and the fluence was kept below 2 μA/cm^2. Homogeneity of irradiations over an area of 10×10 mm^2 was achieved by means of an electronic x-y beam sweep system. During implantation and irradiation the base pressure of the chamber was about 10^{-4} Pa. At least one PAC spectrum was taken after each subsequent irradiation step at room temperature.

The PAC and CEMS methods are described in many textbooks.[9,10] Therefore only some special features of the PAC method are explained here. The PAC probe ^{111}In decays with a half-life of $T_{1/2}=2.8$ d via electron capture to ^{111}Cd. The $5/2^{+}$ intermediate state in the γ cascade in ^{111}Cd (mean life $\tau=122$ ns) senses the hyperfine fields and gives access to the local magnetic field(s) $B_{\rm hf}$ (MHF) and electric field gradient(s) (EFG) via the perturbed angular correlation of two emitted γ radiations. If all probe nuclei are exposed to the same magnetic hyperfine field $B_{\rm hf}$, only the Larmor frequency $\omega_L=\mu B_{\rm hf}/\hbar$ and its first harmonic occur in the perturbation factor,

$$G_2^{\rm magn}(t)=\sum_{n=0}^{2} s_n\cos(n\omega_L t)\exp(-n\delta t)d(n\omega_L,\tau_r), \quad (1)$$

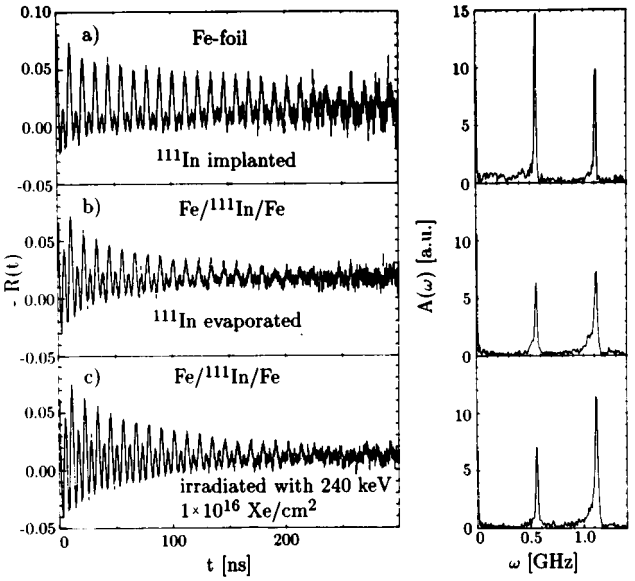

FIG. 1. PAC measurements in Fe: (a) Fe foil after ^{111}In implantation; (b) ^{111}In deposited between two Fe layers; (c) after 240 keV Xe irradiation. Left-hand side: perturbation functions $R(t)$; right-hand side: Fourier spectra $A(\omega)$.

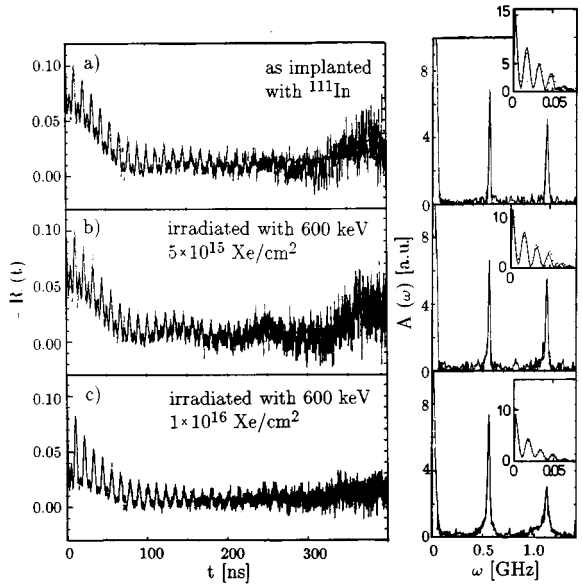

FIG. 2. PAC measurements in the In/Fe bilayer: (a) with ^{111}In implanted; (b) and (c) after 600-keV Xe irradiations. The insets show the Fourier transform also with a better resolution in the low-frequency region.

with $d(\omega,\tau_r)=\exp[-(\omega\tau_r)^2/16\ \ln 2]$ taking into account the finite time resolution of the spectrometer ($\tau_r=1.5$ ns). The coefficients s_n depend on the orientation of the $B_{\rm hf}$ relative to the detector plane.

In the case of pure electric interaction three transition frequencies occur, which are characterized by the coupling constant ν_Q and the asymmetry parameter η. They are correlated to the eigenvalues $V_{\alpha\alpha}$ of the EFG tensor by $\nu_Q=eQV_{zz}/h$ and $\eta=(V_{xx}-V_{yy})/V_{zz}$. In the case of electric interaction $G_2(t)$ is given by

$$G_2^{\rm el}(t)=\sum_{n=0}^{3} s_{2n}(\eta)\cos[g_{2n}(\eta)\nu_Q t]\times\exp[-g_{2n}(\eta)\delta t]d(g_{2n}(\eta)\nu_Q t,\tau_r). \quad (2)$$

There may be a number of inequivalent sites i occupied by PAC probe atoms. With the fractional occupation probability f_i the experimental perturbation function $R(t)$ is given by

$$R(t)=A_{22}^{\rm eff}\sum f_i G_2^{(i)}(t). \quad (3)$$

If electric and magnetic hyperfine interaction are present at the same probe nucleus, combined hyperfine interaction is observed.[11] For the case of a strong magnetic field and a weak EFG, Wenzel, Uhrmacher, and Lieb[12] have recently given a simple approximative formula of the combined hyperfine interaction. All the PAC measurements were performed using a four-detector setup, equipped with BaF_2 scintillation detectors and fast-fast electronics, as described in Ref. 13. The CEMS measurements using the isotope ^{57}Fe were performed using the apparatus described in Ref. 14.

III. EXPERIMENTAL RESULTS

A. PAC measurements in Fe

In Fig. 1, two PAC measurements of ^{111}Cd in Fe obtained immediately after preparation are shown. The upper spectrum [Fig. 1(a)] was taken after the implantation of ^{111}In into an iron foil. A second sample was prepared by evaporation of a 104-nm iron layer onto the silicon substrate. Afterwards ^{111}In was evaporated onto the iron surface and covered with a second (27 nm) layer of iron [Fig. 1(b)]. Both PAC spectra exhibit a pure magnetic signal with the Larmor frequency $\omega_{L0}=560(1)$ MHz and a fraction of $f_0=64(5)\%$ after ^{111}In implantation compared to $f_0=60(5)\%$ after ^{111}In evaporation. This hyperfine field is characteristic of ^{111}Cd probes on defect-free substitutional sites in iron.[15,16] It is obvious that the damping δ of this fraction is smaller when the ^{111}In ions are implanted ($\delta=2.7$ MHz compared to $\delta=7.8$ MHz). The remaining probes experience a second magnetic hyperfine field with a broad frequency distribution ($\delta_3=35$ MHz) and a reduced Larmor frequency of $\omega_{L3}=530(15)$ MHz. The third spectrum in Fig. 1(c) was taken after irradiation of the evaporated film with 1×10^{16} Xe/cm^2 at 240 keV. No further fraction appeared and only a slight decrease of the damping ($\delta_0=6$ MHz) at the substitutional site was found. The two observed PAC fractions f_0 and f_3 are therefore characteristic for ^{111}In(EC)^{111}Cd probes in pure Fe.

B. PAC measurements in a Fe/In bilayer

Figure 2 shows the PAC measurements of a Fe/In bilayer (82-nm In on 100-nm Fe). The upper PAC spectrum [Fig. 2(a)] was taken directly after implantation of ^{111}In. Two almost undamped fractions were found: 39(5)% of the ^{111}Cd atoms were exposed to the MHF of pure Fe, the rest were found to be exposed to an EFG [$\nu_Q=17(1)$ MHz, $\eta=0$], known for ^{111}Cd in In metal.[17] After the first Xe irradiation

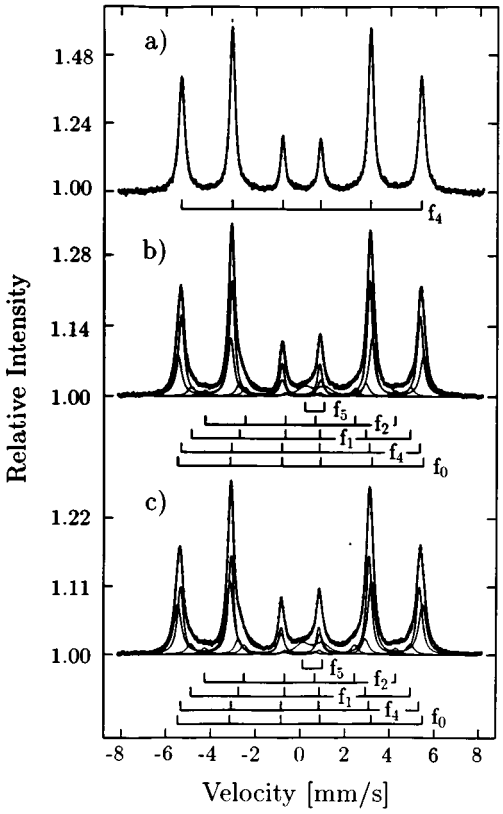

FIG. 3. CEMS spectra of a ^{57}Fe enriched bilayer: (a) as deposited; (b) and (c) mixed at 450 keV with fluences of 2.8×10^{15} and 5.8×10^{15} Xe/cm^2.

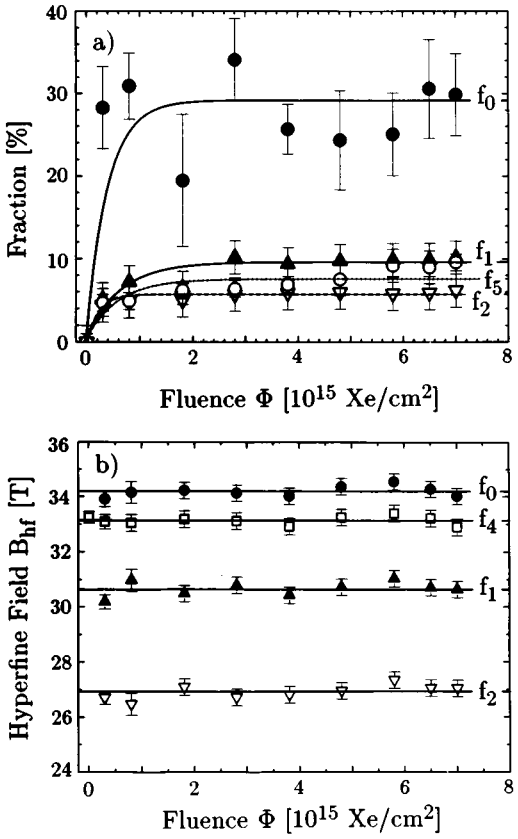

FIG. 4. Fractions (top) and magnetic hyperfine fields B_{hf} (bottom) after Xe irradiations as measured by CEMS.

with 5×10^{15} Xe/cm^2 at 600 keV, only a slight change of the spectrum was observed: in addition to the two substitutional fractions In(^{111}Cd) and Fe(^{111}Cd) a fraction with $f_3=15\%$ and a Larmor frequency of $\omega_{L3}=535(15)$ MHz with $\delta_3=35(15)$ MHz appeared. Further irradiations led to an increase of this fraction ($f_3=35\%$) at the expense of the pure Fe and In signals. Furthermore, a damping of the In(^{111}Cd) signal was observed.

C. PAC and CEMS measurements in the Fe/Ag bilayers and multilayers

For the ^{57}Fe CEMS investigations, samples consisting of 80-nm natural Fe on a silicon substrate were covered with another 13-nm Fe film that was enriched (95%) in ^{57}Fe. Afterwards, these layers were covered with a film of 50-nm Ag. This sample geometry was chosen in order to raise the sensitivity to the Fe/Ag interface. Figure 3(a) shows a CEMS spectrum after preparation. Although an enriched ^{57}Fe layer was used, it was not possible to identify the Fe sites at the Fe/Ag interface. This changed with the Xe irradiation, which became obvious through the changes in the corresponding CEMS spectra displayed in Fig. 3. After irradiation with 450 keV, three other magnetic fractions appeared in addition to the substitutional field of $B_4^{\mathrm{CEMS}}=33.1(3)$ T in α-Fe. Two of them had reduced magnetic fields of $B_1^{\mathrm{CEMS}}=30.3(4)$ T (f_1) and $B_2^{\mathrm{CEMS}}=26.6(3)$ T (f_2), whereas the third fraction (f_0) had a somewhat higher field of $B_0^{\mathrm{CEMS}}=33.9(2)$ T. In addition, a paramagnetic fraction (f_5) was found as a doublet in the spectra. The magnetic hyperfine fields did not change significantly with the irradiation, as can be observed in Fig. 4. The fractions of these additional sites were found to saturate very fast with the implantation dose. In a measurement at 4.2 K, a magnetic splitting of the former doublet fraction with $B_5^{\mathrm{CEMS}}=26.4(6)$ T was observed (Fig. 5).

PAC experiments were carried out on multilayers consisting of four layers of Fe, three layers of Ag (20 nm each), and a Ag layer of 40 nm on top of that sandwich. Figure 6(a) shows the Fourier spectra taken immediately after implantation of ^{111}In and after subsequent irradiations with a dose of 3×10^{15} Xe/cm^2 at an energy of 450 keV [Figs. 6(b) and 6(c)]. Common to all spectra are the frequency components between 400 and 560 MHz (and their first harmonics at 2 ω_L). To get a consistent fit of all data it was necessary to introduce two new fractions f_1 and f_2 with $\omega_{L1}=500(15)$ MHz and $\omega_{L2}=440(25)$ MHz in addition to the fractions f_0 and f_3 already known from the measurements in pure iron. Due to the spontaneous magnetization of the sample it was necessary to fit the individual amplitude factors s_n ($n=0,1,2$), which deviate from the values in a nonmagnetized sample. Unfortunately, the PAC signal for ^{111}Cd in Ag has a vanishing coupling constant $\nu_Q=0$ [Eq. (2)]. Therefore it was not possible to distinguish between the substitutional Ag-site fraction and the s_0 parts of the magnetic fractions [see Eq. (1)]. For this reason, in Fig. 7 the relative magnetic fractions $f_i/\Sigma f_i$ are plotted. The decrease of the substitutional fraction f_0 in favor of the fractions with lower fields f_i ($i=1-3$) is obvious.

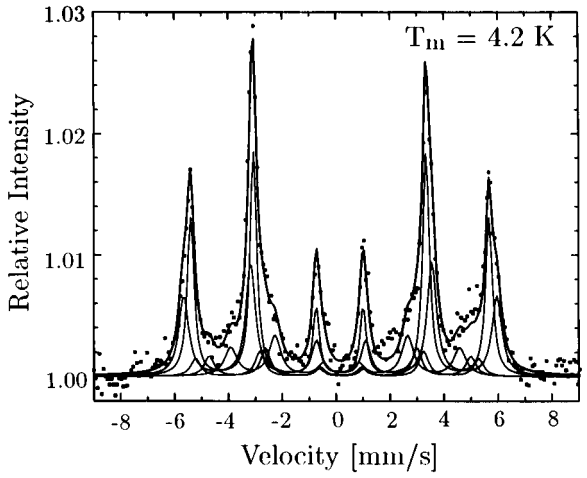

FIG. 5. CEMS spectrum of a ^{57}Fe enriched bilayer after Xe irradiation measured at 4.2 K.

D. Measurements in Fe supersaturated with Ag

As a supplementary measurement, ^{111}In was also implanted into a Fe film, supersaturated with Ag. This sample was laser deposited onto a silicon substrate at room temperature.[18] The homogeneous distribution of the Ag atoms in the film was checked by x-ray diffraction (XRD) and energy dispersive x-ray (EDX) analysis. The PAC spectrum after implantation of a sample with 6% Ag is shown in Fig. 8. In this case, the film was magnetized by an external field of 0.14 T perpendicular to the detector plane. Under such conditions only the higher harmonics $2\omega_L$ appear ($s_0=s_1=0$). The hyperfine parameters for this sample are given in Table I. The slightly reduced ω_{Li} values for all the fractions compared to those found in pure Fe and multilayer experiments (Table II) are remarkable.

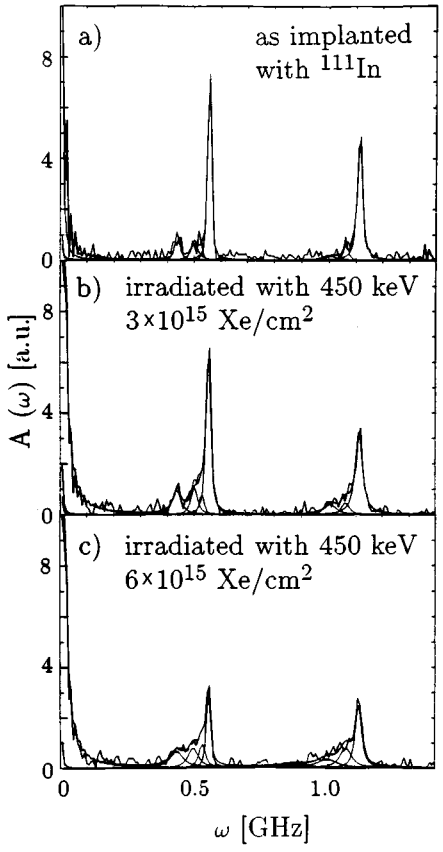

FIG. 6. PAC spectra of an Fe/Ag multilayer: (a) as implanted with ^{111}In; (b) and (c) after 450-keV Xe irradiations.

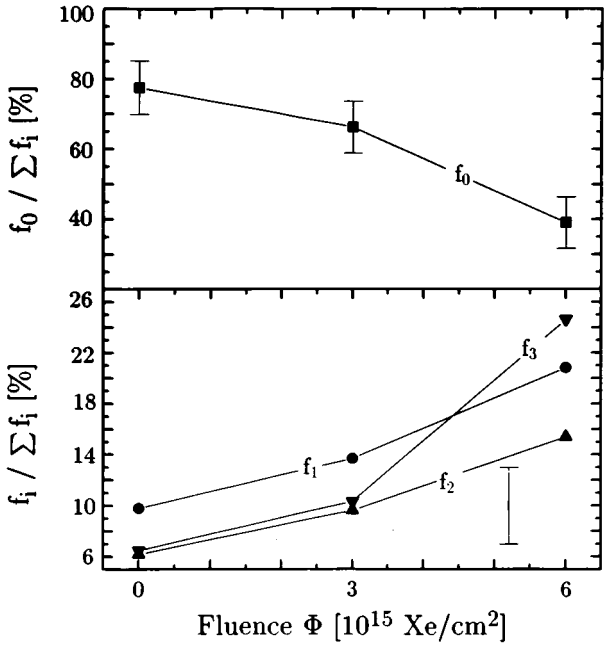

FIG. 7. Fractions after Xe irradiations of the Ag/Fe multilayer obtained by PAC. Typical errors are indicated.

E. Observation of the mixing effect by ^{111}In deposited at the interface

The implantation of ^{111}In with 400 keV results in a Gaussian depth profile of the probe atoms (full width at half maximum of about 75 nm). Therefore, the information obtained from these experiments results from a relatively large volume of the sample. In order to reach a higher sensitivity to the mixing process at the interface, all the 10^{12} ^{111}In atoms were deposited at the Ag/Fe or the In/Fe interface.

After preparation, the PAC signal of the Ag/Fe sample is strongly damped [Fig. 9(a)]. The almost complete absence of typical Fe fractions and the Ag signal ($\nu_Q=0$) indicates that the probes are located at the interface. After Xe irradiation with a dose of 3×10^{15} Xe/cm^2 a drastic change was observed [Fig. 9(b)]: 75% of the probe atoms were exposed to a damped fraction with $\nu_Q=0$. The remaining 25% were exposed to MHF's similar to those found in the Ag/Fe

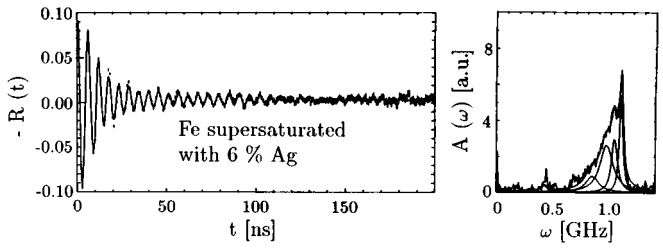

FIG. 8. PAC spectrum of Fe supersaturated with 6% Ag and doped with ^{111}In.

TABLE I. Hyperfine parameters of the Fe sample supersaturated with 6% Ag.

Site i	ω_{Li} (MHz)	δ_i (MHz)	f_i (%)	P (%)
0	553(3)	9(3)	23(6)	42
1	488(15)	34(6)	39(7)	38
2	425(25)	34(7)	17(8)	16
3	523(10)	15(8)	20(8)	

multilayer and the Fe(Ag) alloy. A further irradiation did not change this spectrum significantly.

After preparation of the In/Fe sample, 48(8)% of the ^{111}In atoms are located in an In matrix [Fig. 10(a)]. The remaining probes cannot be associated with pure magnetic nor with pure electric hyperfine interaction. No further information can be obtained from this kind of combined interaction because neither the MHF nor the magnitude or orientation of the EFG are known. After the first irradiation, the substitutional In fraction increased to 79(8)% and the rest was again exposed to combined interaction. In agreement with the Ag/Fe experiment, a second irradiation did not change the spectrum (Fig. 10).

IV. DISCUSSION

A. Site identification

The PAC and CEMS measurements in pure Fe revealed the known MHF's for the substitutional lattice site: $B_4^{\mathrm{CEMS}}=33.1(3)$ T in the case of Fe(^{57}Fe)[19] and $B_0^{\mathrm{PAC}}=38.2(2)$ T for Fe(^{111}Cd).[16] This dependence of the MHF's on the probe nuclei is well known[20] and can be reproduced by calculations that take into account local fluctuations of the spin density.[21,22]

Fraction (f_3) with a Larmor frequency of $\omega_{L3}=530(15)$ MHz appeared in all the samples, even in the pure Fe samples. Therefore, it has to be attributed to a trapped defect next to the probe atom. The damping of this field ($\delta_3=35$ MHz) indicates that in addition to a MHF an EFG is present. In the limit of combined interaction with a very large MHF of $B_3^{\mathrm{PAC}}=36.1(7)$ T, the magnetic interaction dominates the spectrum and the EFG will only generate the line broadening in the Fourier spectrum. Using the approximation of Ref. 12, the strength of the EFG can be estimated from the distribution width, corresponding to $\nu_Q\approx 45$ MHz. The structure of this defect has not yet been analyzed.

The CEMS measurements performed at 293 K after Xe irradiation revealed two fractions with reduced MHF's [$B_1^{\mathrm{CEMS}}=30.3(4)$ T and $B_2^{\mathrm{CEMS}}=26.6(3)$ T]. In α-Fe, impurity atoms are known to cause such a reduction of the MHF, which increases with the number of impurities next to the probe. This has, for example, been shown for Al, Si, Mn, V, and Cr.[23] For these reasons, we identify B_1^{CEMS} with one and B_2^{CEMS} with two Ag atoms next to the ^{57}Fe probe. In analogy, B_1^{PAC} and B_2^{PAC} are attributed to one and two Ag atoms in next-neighbor positions to the ^{111}In.

In the CEMS experiments in addition to the two reduced MHF's the field $B_0^{\mathrm{CEMS}}=33.9(2)$ T was found, which is slightly larger than the substitutional one. This is typical for a widened Fe lattice.[24,25] For Fe(Ag) alloys such a widening by substitutional dissolved Ag has indeed been proven.[18,26] Therefore, this fraction is attributed to ^{57}Fe probes in an Fe lattice, which is expanded by Ag atoms, but does not have any direct Ag neighbors.

Referring to Schurer, Celinski, and Heinrich,[27] the paramagnetic fraction f_5 has to be attributed to Fe atoms in the Ag matrix. These authors observed a ferromagnetic ordering and an increase of the Curie temperature T_C with the Fe concentration. The mean isomer shift of the doublet $\delta=0.33(9)$ mm/s indicates a Fe concentration of about 15(8) at. % in the Ag matrix. The magnetic splitting at 4.2 K proves this identification.

The measurements in the Ag-supersaturated Fe sample gave an ideal opportunity to test the proposed identifications. As the sample had a homogeneous Ag content of 6%, the probability that the probe is surrounded by a certain number of Ag atoms can be calculated using a binomial distribution. Because of the only slightly different distance (15%) to the probe site the eight nearest and six next-nearest neighbors were regarded as ''next neighbors.'' The probabilities P for none, one, and two Ag atoms to be in next neighborhood of the ^{111}In probe is given in the last column of Table I. Comparing these probabilities with the experimental fractions, perfect agreement was found for fractions f_1 and f_2. Finally, also the probability of $P=42\%$ for the probes having no Ag neighbors is reproduced when the defect associated fraction f_3 is added to the substitutional fraction f_0.

In the Fe(Ag) films prepared by laser deposition, Störmer, Krebs, and Fähler[28] measured a high stress of ≈ 3 GPa via XRD. The pressure dependence of the MHF for ^{111}Cd in Fe has been investigated by Lindgren and Vijay,[15] who found a decrease of the MHF with increasing pressure. This seems to be reasonable for the slightly lower Larmor frequencies in the measured alloy (compare Tables I and II). In agreement

TABLE II. Magnetic hyperfine fields measured at room temperature with PAC and CEMS (n denotes the number of Ag neighbors next to the probe).

			PAC		CEMS	
	f_i	ω_{Li} (MHz)	B_i^{PAC} (T)	B_i^{PAC}/B_0	B_i^{CEMS} (T)	B_i^{CEMS}/B_0
α-Fe(Ag) $n=0$	f_0	560(2)	38.2(2)	1.00	33.9(2)	1.00
α-Fe(Ag) $n=1$	f_1	500(15)	34.1(10)	0.89(3)	30.3(4)	0.89(1)
α-Fe(Ag) $n=2$	f_2	440(25)	30.0(17)	0.79(5)	26.6(3)	0.79(1)
α-Fe+defect	f_3	530(10)	36.1(7)	0.95(2)		
α-Fe	f_4				33.1(3)	0.98(1)

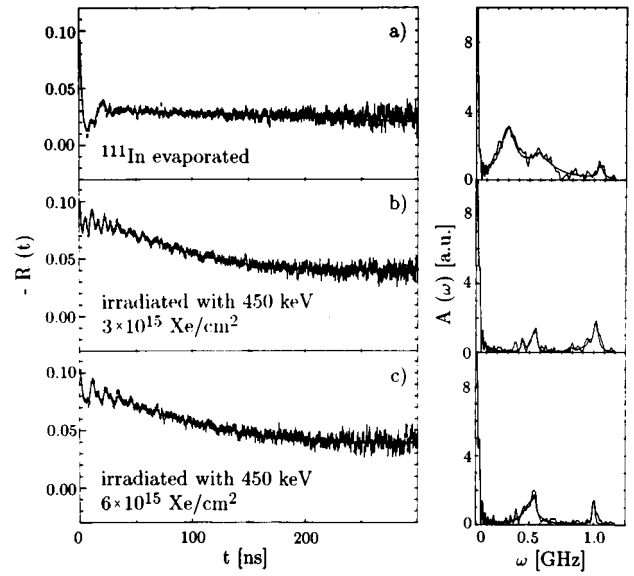

FIG. 9. PAC spectra of an Ag/Fe bilayer. ^{111}In was deposited at the interface by thermal evaporation. (a) as deposited; (b) and (c) irradiated with 450 keV ions.

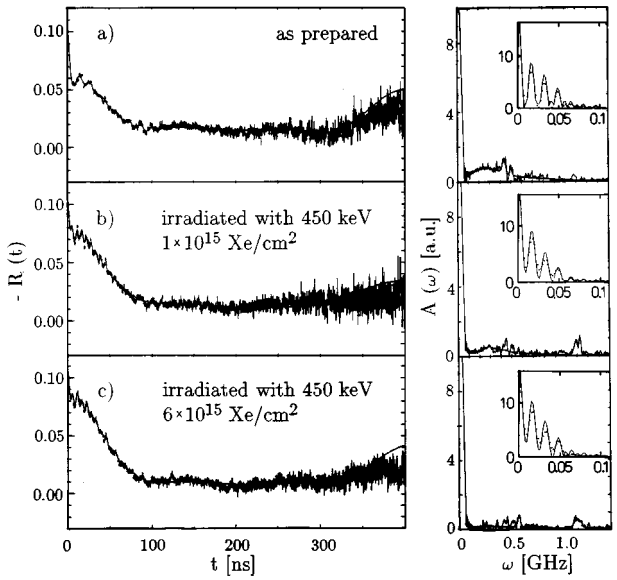

FIG. 10. PAC spectra of an In/Fe bilayer. ^{111}In was deposited at the interface by thermal evaporation. (a) as deposited; (b) and (c) irradiated with 450 keV ions. The insets show the Fourier transform also with a better resolution in the low-frequency region.

with the XRD measurements, a stress of 3(2) GPa can be calculated from the reduced MHF's.

For a comparison of the PAC and CEMS results, the relative decrease of the MHF is considered (Table II): The fields measured by PAC were normalized to the substitutional field $B_0^{\mathrm{PAC}}=38.2(2)$ T, and the fields measured by CEMS to the value for ^{57}Fe in the Ag-enriched area $B_0^{\mathrm{CEMS}}=33.9(2)$ T. Surprisingly, in this case the relative MHF's found with both methods are in perfect agreement. This can be understood if one realizes that the ^{111}In probe itself is a foreign atom in the Fe lattice, which may cause a small dilatation of its own neighborhood. Therefore the ''substitutional'' PAC site in Fe seems to correspond to the widened Fe lattice in the CEMS measurements. The fact that the defect-associated fraction f_3 only occurs in the PAC investigations also hints at such a small lattice distortion caused by the ^{111}In itself. This distortion may lead to an attractive interaction between the ^{111}In probe and dilute defects which cannot be observed by CEMS.

B. Mixing

In the miscible systems Ni/Sb and Ni/Al it has been shown that after low fluence Xe irradiation of 5×10^{15} Xe/cm^2 the multilayers were fully mixed and crystalline intermetallic phases had been formed,[6,7] as proven by PAC, XRD, and transmission electron microscopy (TEM). Obviously, this is not the case for the immiscible systems Ag/Fe and In/Fe. Neither in the CEMS nor in the PAC experiments was phase formation detected. Nevertheless, the site identification of the different fractions proved that after irradiation at a fluence of $10^{15}-10^{16}$ Xe/cm^2, Ag atoms are found in the Fe-matrix fractions (f_1 and f_2). From the CEMS measurements it can be concluded that also few Fe atoms remain in the Ag lattice (f_5). Such a small mixing efficiency was not observed for miscible systems consisting of heavy elements ($\overline{Z}>20$), for which mixing by thermal spikes is expected. We therefore propose that the large ΔH_{mix} is reponsible for the low mixing efficieny observed.

Further information on the mixing process was obtained from the PAC measurements, where ^{111}In was deposited directly at the interface. After the first irradiation, 75% of the ^{111}In atoms were found in the Ag lattice and only 25% were exposed to MHF's. This is in contrast to ballistic simulations with the computer code TRIM.[29] They predict that 70% of the ^{111}In atoms are transported into the Fe layer and only 30% into the Ag layer. But if chemistry governs the mixing mechanism at the interface, then ^{111}In is expected to diffuse into Ag because, according to the phase diagrams, In is miscible with Ag but not with Fe. From this we also conclude that the mixing process at the interface is not determined by ballistic collisions, but by chemical driving forces. This conclusion is further supported by the fact that the second irradiation did not change the spectrum (see Fig. 9) as thermal spikes at the interface led to a phase separation.

Likewise, in the PAC experiments where ^{111}In had been deposited at the In-Fe interface, no significant amount of ^{111}In was found in Fe and a second irradiation did not change this situation.

V. CONCLUSIONS

We have investigated the hyperfine interaction of ^{111}In and ^{57}Fe nuclei in Xe-irradiated Ag/Fe and In/Fe layered structures via PAC and CEMS. Various layer geometries (bilayer, multilayers) have been studied, and the ^{111}In tracers were either deposited at the interface or introduced via ion implantation. For comparison, measurements have also been performed in a supersaturated Fe(Ag) alloy.

The results obtained with both types of hyperfine techniques are very consistent insofar as identical fractions with different magnetic hyperfine fields have been identified. We

associate one fraction with defects in Fe and three fractions with microsurroundings of Ag atoms in the vicinity of the probe atoms in Fe. The ratios of hyperfine fields for these ''Ag-decorated'' probes relative to those of the nondecorated probes are in perfect agreement for PAC and CEMS. A slight effect of lattice distortion via the PAC probe atom itself or via Ag atoms in the Fe matrix has been observed.

While we have been able to identify the structures and fractions of these point defects, we did not find evidence for the formation of intermetallic phases near the interface. In this respect our findings are consistent with the positive heat of mixing in the Ag/Fe and In/Fe systems, which would forbid such intermetallic compounds to be formed in thermal equilibrium. The ballistic atomic mixing via collision cascades seems to be counterbalanced by the demixing occurring in the thermal spike phase of the irradiation process. Crespo-Sosa and co-workers[30] have recently performed combined RBS and scanning tunneling microscopy for Ag/Fe bilayers irradiated with Ar and Xe ions at liquid nitrogen temperature in order to monitor the interface broadening and surface roughening induced by the ion beam bombardment. These authors also came up with very small interface mixing rates that are, indeed, smaller than expected from ballistic mixing and again indicate demixing and phase separation near the interface. Taking into account all these arguments, we conclude that the ion beam induces long-range transport of few Ag atoms into Fe (and Fe atoms into Ag) as a consequence of ballistic transport, while the short-range transport is counterbalanced by the thermal spike demixing process. It would therefore be very useful to experimentally differentiate between the length scales of the two processes.

ACKNOWLEDGMENTS

The authors are grateful to D. Purschke for expertly running the IONAS accelerator, to Dr. H.U. Krebs for providing us with the homogeneous Fe(Ag) alloy, and to Dr. W. Bolse for illuminating discussions. Finally, we would like to thank Dr. Ph. Bauer, University of Nancy, who carried out the 4.2-K measurement and Dr. C. Tosello, University of Trento, for preparing the enriched ^{57}Fe samples.

[1] W. Bolse, Mater. Sci. Eng. **R12**, 53 (1994).
[2] P. Sigmund and A. Gras-Marti, Nucl. Instrum. Methods **168**, 389 (1980).
[3] P. Sigmund and A. Gras-Marti, Nucl. Instrum. Methods. **182/183**, 25 (1981).
[4] P. Borgensen, T. L. Lilienfeld, and H. H. Johnson, Appl. Phys. A **50**, 161 (1990).
[5] Y. T. Cheng, Mater. Sci. Rep. **5**, 45 (1990).
[6] T. Weber and K. P. Lieb, J. Appl. Phys. **73**, 3499 (1993).
[7] M. Uhrmacher, P. Wodniecki, F. Shi, T. Weber, and K. P. Lieb, Appl. Phys. A **57**, 353 (1993).
[8] G. Principi, in *Mössbauer Spectroscopy Applied to Magnetism and Material Science*, edited by G. J. Long and F. Grandjean (Plenum, New York, 1994).
[9] G. Schatz and A. Weidinger, *Nukleare Festkörperphysik* (Teubner, Stuttgart, 1992).
[10] H. Frauenfelder and R. M. Steffen, in *Alpha-, Beta-, Gamma-Ray-Spectroscopy*, edited by K. Siegbahn (North-Holland, Amsterdam, 1965).
[11] K. Alder, E. Matthias, W. Schneider, and R. M. Steffen, Phys. Rev. **129**, 1199 (1963).
[12] T. Wenzel, M. Uhrmacher, and K. P. Lieb, J. Phys. Chem. Solids **55**, 683 (1994).
[13] A. Bartos, K. Schemmerling, T. Wenzel, and M. Uhrmacher, Nucl. Instrum. Methods A **330**, 132 (1993).
[14] P. Schaaf, T. Wenzel, K. Schemmerling, and K. P. Lieb, Hyperfine Interact. **92**, 1189 (1994).
[15] B. Lindgren and Y. K. Vijay, Hyperfine Interact. **9**, 379 (1981).
[16] F. Pleiter, C. Hohenemser, and A. R. Arends, Hyperfine Interact. **10**, 691 (1981).
[17] R. Vianden, Hyperfine Interact. **15-16**, 1081 (1983).
[18] H. U. Krebs, S. Fähler, M. Störmer, A. Crespo-Sosa, P. Schaaf, and W. Bolse, Appl. Phys. A **61**, 591 (1995).
[19] R. S. Preston, S. S. Hanna, and J. Heberle, Phys. Rev. **128**, 2207 (1962).
[20] G. N. Rao, Hyperfine Interact. **26**, 1119 (1985).
[21] S. Blügel, H. Akai, R. Zeller, and P. H. Dederichs, Phys. Rev. B **35**, 3271 (1987).
[22] J. Kanamori, H. K. Yoshoa, and K. Terakura, Hyperfine Interact. **9**, 363 (1981).
[23] M. B. Stearns, Phys. Rev. **147**, 439 (1966).
[24] E. Kneller, *Ferromagnetism* (Springer, Berlin-Göttingen, 1962).
[25] P. Schaaf, G. Rixecker, E. Yang, C. N. J. Wagner, and U. Gonser, Hyperfine Interact. **94**, 2239 (1994).
[26] K. Sumiyama and Y. Nakamura, in *Rapidly Quenched Metals*, edited by S. Steeb and H. Warlimont (Elsevier, New York, 1985).
[27] P. J. Schurer, Z. Celinski, and B. Heinrich, Phys. Rev. B **51**, 2506 (1995).
[28] M. Störmer, H. U. Krebs, and S. Fähler (private communication).
[29] J. P. Biersack and L. G. Haggmark, Nucl. Instrum. Methods B **50**, 257 (1990).
[30] A. Crespo-Sosa, P. Schaaf, W. Bolse, K. P. Lieb, M. Gimbel, U. Geyer, and C. Tosello, Phys. Rev. B (to be published).